MCB
Journals.ASM.org

DHHC17 Palmitoylates ClipR-59 and Modulates ClipR-59 Association with the Plasma Membrane

Wenying Ren,[a] Yingmin Sun,[a,b] Keyong Du[a]

Molecular Oncology Research Institute, Tufts Medical Center, Boston, Massachusetts, USA[a]; China Agricultural University College of Biological Science, Beijing, China[b]

ClipR-59 interacts with Akt and regulates Akt compartmentalization and Glut4 membrane trafficking in a plasma membrane association-dependent manner. The association of ClipR-59 with plasma membrane is mediated by ClipR-59 palmitoylation at Cys534 and Cys535. To understand the regulation of ClipR-59 palmitoylation, we have examined all known mammalian DHHC palmitoyltransferases with respect to their ability to promote ClipR-59 palmitoylation. We found that, among 23 mammalian DHHC palmitoyltransferases, DHHC17 is the major ClipR-59 palmitoyltransferase, as evidenced by the fact that DHHC17 interacted with ClipR-59 and palmitoylated ClipR-59 at Cys534 and Cys535. By palmitoylating ClipR-59, DHHC17 directly regulates ClipR-59 plasma membrane association, as ectopic expression of DHHC17 increased whereas silencing of DHHC17 reduced the levels of ClipR-59 associated with plasma membrane. We have also examined the role of DHHC17 in Akt signaling and found that silencing of DHHC17 in 3T3-L1 adipocytes decreased the levels of Akt as well as ClipR-59 on the plasma membrane and impaired insulin-dependent Glut4 membrane translocation. We suggest that DHHC17 is a ClipR-59 palmitoyltransferase that modulates ClipR-59 plasma membrane binding, thereby regulating Akt signaling and Glut4 membrane translocation in adipocytes.

ClipR-59 is a plasma membrane (PM)-associated protein characterized with three ankyrin repeats at the amino terminus, two putative cytoskeleton-associated protein glycine-rich (CAP-Gly) domains in the middle, and a membrane binding domain (MBD) at the carboxyl terminus (1). Recent studies revealed that ClipR-59 is a modulator of Akt signaling in that ClipR-59 interacts with active Akt and modulates Akt intracellular compartmentalization (2). Moreover, ClipR-59 was also found to interact with AS160, a Rab GTPase-activating protein that modulates Glut4 membrane translocation (3). In this context, ClipR-59 functions as a scaffold protein to facilitate AS160 phosphorylation by Akt and subsequently insulin-dependent Glut4 membrane translocation (4). Glut4 is the major mediator of insulin-induced glucose disposal from circulation and has a fundamental role in maintenance of body glucose homeostasis and regulation of peripheral insulin sensitivity (5, 6). In mice, inactivation of Glut4 in either muscle or adipocytes causes severe glucose intolerance and hepatic insulin resistance (7–9). In this regard, ClipR-59 is believed to play a role in the regulation of body glucose homeostasis and peripheral insulin sensitivity.

The modulation of the Akt PM association by ClipR-59 requires two functional features of ClipR-59: interaction with Akt and PM localization. In adipocytes, the form of ClipR-59 defective in either Akt interaction or PM binding failed to recruit Akt onto the PM (2). ClipR-59 PM binding is, in part, mediated by palmitoylation of cysteine residues at 534 and 535 within the MBD (10). Therefore, it is believed that modulation of ClipR-59 palmitoylation may constitute a critical process for ClipR-59 to regulate Akt signaling.

In eukaryotes, protein palmitoylation at cysteine residues is catalyzed by DHHC palmitoyltransferase, which is so named because all palmitoyltransferases consist of an aspartic acid-histidine-histidine-cysteine (DHHC) motif within their catalytic domain (11, 12). There are a total of 23 DHHC palmitoyltransferases in mammals (13). In the present study, we tested the hypothesis that one or more DHHC proteins among these 23 palmitoyltransferases may function as ClipR-59 palmitoyltransferase and have identified DHHC17 as the ClipR-59 palmitoyltransferase. Moreover, we found that, by modulating ClipR-59 palmitoylation, DHHC17 contributes to the regulation of Akt signaling and insulin-dependent Glut4 membrane translocation.

MATERIALS AND METHODS

Reagents. Insulin, dexamethasone (Dex), 3-isobutyl-1-methylxanthine (IBMX), hydroxylamine chloride, rabbit anti-syntaxin 4 and DHHC17 antibodies, and mouse monoclonal anti-Flag antibody were from Sigma. Thiopropyl Sepharose 6B and glutathione-Sepharose 4B were from GE Healthcare. Methyl methanethiosulfonate (MMTS), rabbit anti-Glut4, mouse anti-green fluorescent protein (anti-GFP), and anti-glutathione *S*-transferase (anti-GST) antibodies were from Thomas Scientific. Mouse monoclonal antihemagglutinin (anti-HA) antibody was from Covance. Mouse monoclonal anti-Glut4 antibody (1F8) and rabbit monoclonal Akt, phospho-Akt, and IRAP antibodies were from Cell Signaling. Rabbit anti-ClipR-59 antibody has been described previously (2).

Plasmids and virus production. ClipR-59 and its mutants have been described previously (2). HA-tagged murine DHHC protein expression vectors and internal HA-tagged Glut4 expression vector were kindly provided by Masaki Fukata and Samuel W. Cushman, respectively (14). Two sets of DHHC17 short hairpin RNA (shRNA) were used in this study. One DHHC17 shRNA was generated according to the published sequence (15, 16), and the other one (TRCN0000137952) was purchased from Sigma. GST-DHHC17 expression vector pEBG-DHHC17 was generated via inserting DHHC17 into the BamHI and NotI sites of pEBG. GFP-MBD was generated via inserting the MBD domain of ClipR-59 into BglII and XhoI sites of pEGFP-C1. To generate the expression vector that simultaneously

Received 30 April 2013 Returned for modification 29 May 2013
Accepted 21 August 2013
Published ahead of print 3 September 2013
Address correspondence to Keyong Du, kdu@tuftsmedicalcenter.org.

doi:10.1128/MCB.00527-13

expresses shRNA and GFP–ClipR-59, DHHC17 shRNA and luciferase shRNA were excised from pLKO with NotI and EcoRI sites and the NotI site was blunted and inserted into the MfeI and NruI sites of pcDNA3.0. Then, GFP–ClipR-59 fusion cDNA was cloned into the EcoRV and NotI sites of the resultant shRNA pcDNA3.0 vectors. In this construct, the U6 promoter was in the direction opposite that of the cytomegalovirus (CMV) promoter of pcDNA3.0. The adenoviruses expressing HA-DHHC17 and DHHC17 shRNA were generated and purified by the use of a double-CsCl gradient as described previously (17).

Cell culture and transient transfection. HEK293 and COS-7 cells were grown in high-glucose Dulbecco's modified Eagle's medium (DMEM) with 10% (vol/vol) fetal bovine serum (FBS), 2 mM L-glutamine, 100 U/ml penicillin, and 100 μg/ml streptomycin (Invitrogen). 3T3-L1 preadipocytes were grown in the same DMEM but with 10% bovine serum instead of FBS. The adipocyte differentiation of 3T3-L1 preadipocytes was as described. Briefly, 3T3-L1 preadipocytes were cultured for 2 additional days after reaching 100% confluence and treated with differentiation medium (DMEM-high glucose containing 10% FBS, 2.5 μg/ml insulin, 0.5 mM IBMX, 2.5 μM Dex, 2 mM L-glutamine, 100 units/ml penicillin, 100 μg/ml streptomycin) for 4 days. Then the differentiation medium was changed to the regular medium. After 7 days of differentiation, the adipocytes were used for experiments. When the cells were infected with viruses, at least 75% of cells were transduced.

Metabolic labeling with [^{3}H]palmitate. The metabolic labeling was essentially carried out as described previously (10, 18). Briefly, HEK293 cells in a 6-cm-diameter dish cotransfected with Flag-tagged ClipR-59 and individual DHHC protein expression vectors were incubated with DMEM supplemented with 0.25 mCi/ml [^{3}H]palmitate (PerkinElmer) and 5 mg/ml bovine serum albumin (BSA) for 6 h. The total cell lysates were then prepared and subjected to immunoprecipitation (IP) with anti-Flag antibody. The anti-Flag immunoprecipitates were separated on SDS-PAGE. The gel was fixed, treated with Amplify fluorographic reagent (GE Heathcare), vacuum dried, and exposed to X-ray film (Pierce).

Cell imaging. The cells grown on coverslips were either transfected or infected with the indicated expression vectors. Then the cells were fixed and stained with primary antibodies followed by cyanine (Cy)-conjugated goat anti-mouse or -rabbit secondary antibodies. The fluorescence imaging was captured with confocal microscopy (Olympus).

Subcellular fractionation assay. 3T3-L1 adipocytes, with or without insulin treatment, were suspended into HES I buffer (0.25 M sucrose, 20 mm Tris [pH 7.6], and 1 mM EDTA plus a protease inhibitor mixture set). The cells were homogenized by passage through a 23-gauge needle 10 times, and then the homogenates were centrifuged at 19,000 × *g* for 20 min. To isolate the membrane fraction, the resultant pellets from the 19,000 × *g* centrifugation were layered on HES II buffer (1.12 M sucrose, 20 mM Tris [pH 7.6], 1 mM EDTA) and centrifuged at 100,000 × *g* for 60 min. The resulted pellets were designated the nuclear and mitochondrial fractions. The plasma membrane layers were removed from the sucrose cushion, suspended into HES I buffer, and centrifuged at 41,000 × *g* for 20 min. The resultant pellets represented the plasma membrane (PM). To isolate lipid rafts (or plasma membrane microdomains), the PM were suspended into HES I buffer supplemented with 1% Triton X-100 and centrifuged at 14,000 × *g* for 20 min. The resulted pellets represented lipid raft. To isolate low-density microsomes (LDM), the resultant supernatant from the 19,000 × *g* centrifugation was centrifuged at 175,000 × *g* for 75 min, and the pellets were collected as LDM. The supernatant from the 175,000 × *g* centrifugation was saved and designated the cytosol.

For the screening of ClipR-59 palmitoyltransferase, COS-7 or HEK293 cells were cotransfected with Flag-tagged ClipR-59 expression vectors and individual HA-tagged DHHC protein expression vectors. At 36 to 40 h posttransfection, the cell membrane was prepared for Western blot analysis with anti-Flag antibody.

Coimmunoprecipitation (co-IP) assay. HEK293 or COS-7 cells were cotransfected with Flag–ClipR-59 and HA-DHHC expression vectors (e.g., pEB-HA-DHHC17). Then total cell lysates were prepared in immunoprecipitation buffer (20 mM Tris [pH 7.6], 150 mM NaCl, 0.5 mM EDTA, 0.5 mM dithiothreitol [DTT], 1% NP-40, 10% glycerol, protease and phosphatase inhibitors) and incubated overnight with primary antibodies (i.e., anti-Flag M2 affinity gel or anti-HA or anti-GFP antibodies) followed by 45 to 120 min of incubation with protein A- or G- agarose (depending on the experiments). Immunoprecipitates bound to agarose beads were washed and subjected to SDS-PAGE and Western blot analysis.

Assay of TPC of S-acylated protein. The principle and detailed procedure of the assay of thiopropyl captivation (TPC) of S-acylated protein have been described previously (19, 20). Briefly, the cells were lysed into lysis buffer (20 mM HEPES [pH 7.4], 1 mM EDTA, 1.7% Triton X-100). The genomic DNA and insoluble fraction were removed by spinning the cell lysates at 14,000 × *g* for 10 min. Then the total lysates were diluted into 2× blocking buffer (200 mM HEPES [pH 7.4], 200 mM NaCl, 2 mM EDTA, 5% SDS, 2 μl/ml MMTS) and incubated at 42°C for 15 min. After the total proteins were precipitated with 70% acetone, the precipitated proteins were resuspended into binding buffer.

GST pulldown assay. Total cell lysates prepared from the cells that were transfected with GST expression vectors, and the protein expression vectors indicated in the figure legends were incubated with glutathione beads in co-IP buffer for 2 to 4 h. Then the beads were washed three times with co-IP buffer, and the proteins retained on the glutathione beads were separated on SDS-PAGE and probed with proper antibodies.

Western blotting. After the indicated treatments, cells were washed twice with PBS and extracted with cell lysis buffer (20 mM Tris [pH 7.6], 150 mM NaCl, 0.5 mM EDTA, 0.5 mM DTT, 10 mM β-glycerophosphate, 10% glycerol, protease inhibitors). For cellular fractionation experiments, the cellular fractions were directly dissolved into lysis buffer. Equal amounts of protein were subjected to SDS-PAGE and transferred to nitrocellulose membranes (Bio-Rad). After blocking in 5% dry milk, the membranes were incubated with each primary antibody, followed by incubation with a horseradish peroxidase-conjugated secondary antibody. The protein bands were visualized using an ECL detection system (Pierce). The quantification of the Western blot analysis was determined with Image J software.

Statistical analysis. Means ± standard deviations (SD) were calculated, and statistically significant differences among groups were determined by one-way analysis of variance followed by *post hoc* comparisons or a two-tailed unpaired Student's *t* test for comparisons between two groups, as appropriate. An effect was considered significant when P was <0.05.

RESULTS

Palmitoylation of ClipR-59 is required for ClipR-59 to promote Akt PM association. ClipR-59 PM binding is mediated by palmitoylation at Cys533 and Cys534 (10). To assess the role of ClipR-59 palmitoylation in Akt PM recruitment, we substituted both Cys534 and Cys535 with alanine residues. First, we examined subcellular localization of the resulted palmitoylation-defective ClipR-59 mutant (designated C2A2–ClipR-59) in HEK293 cells. As shown in Fig. 1a, C2A2–ClipR-59 exhibited a reduced PM association compared with wild-type ClipR-59 as previously reported (10).

To determine the impact of C2A2–ClipR-59 on Akt PM association, HEK293 cells transiently transfected with either wild-type or C2A2–ClipR-59 were stimulated with 10 nM insulin for 30 min. Then the PM was prepared for Western blot analysis with anti-phospho-Akt and Akt antibodies. Cells transiently transfected with an empty vector were used as controls. As shown in Fig. 1b, insulin treatment increased the PM levels of phospho-Akt and Akt, respectively (panels i and ii, compare lanes 1 and 2). Ectopic expression of ClipR-59 further increased the levels of phospho-Akt and Akt in PM (Fig. 1b, panels i and ii, compare

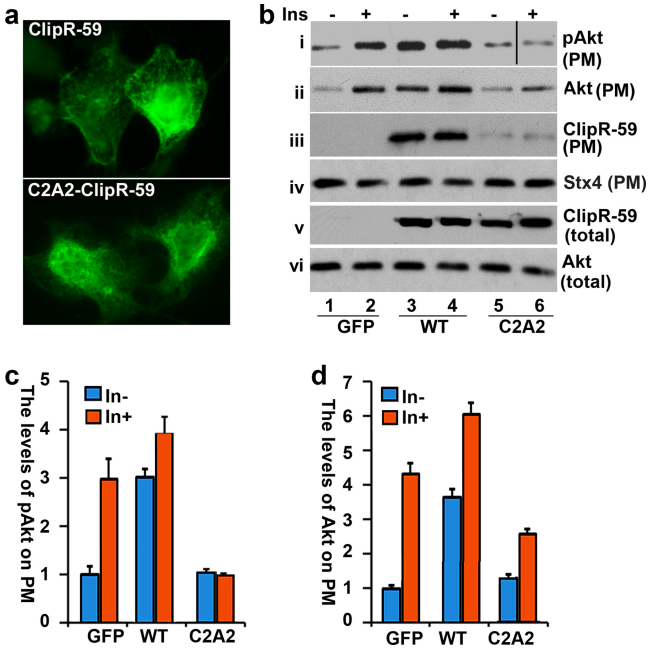

FIG 1 ClipR-59 palmitoylation at Cys534 and Cys535 is required for ClipR-59 to regulate Akt membrane association. (a) Cellular localization of wild-type and palmitoylation-defective C2A2–ClipR-59. HEK293 cells were transiently transfected with Flag-tagged ClipR-59 expression vectors and stained with mouse anti-Flag monoclonal antibody followed by Cy2-conjugated secondary antibodies. (b) The impact of palmitoylation-defective ClipR-59 on Akt PM association. HEK293 cells were transiently transfected with either empty vector or with Flag-tagged ClipR-59 or C2A2–ClipR-59. PM fractions were prepared after the cells were treated with 10 nM insulin (Ins) and subjected to Western blot analysis with anti-phospho-Akt (i), anti-Akt (ii), anti-Flag (iii, for detecting ClipR-59), or anti-syntaxin 4 (iv) (Stx4) antibodies. The total cellular levels of Flag–ClipR-59 (v) and Akt (vi) are also shown. These experiments were repeated three times, and data from one representative experiment are shown. WT, wild type. (c and d) Quantitative presentation of the levels of pAkt and Akt as described for panel b, respectively. The levels of Akt or pAkt were set to a value of 1 in the cells expressing empty vectors without insulin treatment (In−) after normalization to the syntaxin 4 level. Bar graphs show means ± SD ($n = 3$).

lanes 1 and 3) as previously reported in a study demonstrating that ClipR-59 interacts with active Akt and promotes active Akt on PM (2). However, expression of C2A2–ClipR-59 had no such effect (Fig. 1b, panel i, compare lanes 1 and 5) and appeared to cause a decrease in the levels of Akt associated with PM following insulin stimulation (compare lanes 2 and 6 in panels i and ii). Expression of C2A2–ClipR-59 had no impact on Akt expression, as comparable levels of Akt in total cellular homogenates were observed in all samples (Fig. 1b, panel vi). We also examined the level of ClipR-59 on PM. While wild-type ClipR-59 is abundant in PM, only a minimal amount of C2A2–ClipR-59 was detected in the PM fraction (Fig. 1b, panel iii, compare lanes 3 and 4 and lanes 5 and 6), in agreement with the view that ClipR-59 palmitoylation is required for ClipR-59 PM association. The changes in the levels of Akt and ClipR-59 in PM were not the result of sample variations, as comparable levels of syntaxin 4 (Stx4) (Fig. 1b, panel iv), whose membrane association is not regulated, and of total cellular Flag–ClipR-59 (panel v) were observed in each sample. Quantitative analysis of the Western blot shown in Fig. 1b is presented in Fig. 1c and d, which clearly show that C2A2–ClipR-59 lacks the ability to promote Akt PM association. Taken together, these data demonstrate that ClipR-59 palmitoylation is essential for ClipR-59 PM localization and for ClipR-59 to promote Akt PM association.

DHHC17 mediates ClipR-59 palmitoylation. Following the demonstration that ClipR-59 palmitoylation is required for ClipR-59 to regulate Akt PM association, we next attempted to identify the potential ClipR-59 palmitoyltransferase. Since cysteine palmitoylation is catalyzed by DHHC palmitoyltransferase in eukaryotes (11), we reasoned that one or more of mammalian DHHC proteins might be responsible for ClipR-59 palmitoylation. Because ClipR-59 palmitoylation is required for ClipR-59 PM association (Fig. 1; see also reference 10), one could expect that a DHHC protein that promotes ClipR-59 palmitoylation would increase the amount of ClipR-59 associated with PM. With this in mind, we assessed each of the 23 mammalian DHHC palmitoyltransferases with respect to their ability to modulate the association of ClipR-59 with PM in both HEK293 and COS-7 cells. As shown in Fig. 2a, although individual DHHC proteins affected the amount of ClipR-59 associated with PM to different degrees, DHHC13 and -17 (DHHC13 is DHHC22 in reference 14) were particularly effective, as they increased the amount of ClipR-59 associated with PM by more than 10-fold compared with the control (lane 0).

To determine whether the increased ClipR-59 PM association shown by DHHC proteins is indeed related to palmitoylation of ClipR-59, metabolic labeling experiments using ClipR-59 with [^{3}H]palmitate in the presence or absence of exogenously expressed DHHC proteins in HEK293 cells were performed. As shown in Fig. 2b, forcing expression of either DHHC17 or DHHC13 increased the incorporation of [^{3}H]palmitate in ClipR-59 (top panel) without altering ClipR-59 expression (middle panel), arguing that promotion of ClipR-59 PM association by DHHC17 or DHHC13 is directly correlated with their ability to promote ClipR-59 palmitoylation.

Next, palmitoylation of ClipR-59 was assessed by assaying thiopropyl captivation (TPC) of S-palmitoylated protein in the presence or absence of exogenously expressed DHHC17 or DHHC13. As shown in Fig. 2c, ClipR-59 was captured by thiopropyl beads following only hydroxylamine (HyA) treatment and not NaCl treatment (panel i, compare lane 1 and 2), further demonstrating that ClipR-59 is a palmitoylated protein. Forcing expression of either DHHC17 or DHHC13 increased the amount of ClipR-59 captured with thiopropyl beads under conditions of hydroxylamine treatment (Fig. 2c, panel i, compare lanes 2, 4, and 6), providing additional evidence that DHHC17 and DHHC13 promote ClipR-59 palmitoylation. In these experiments, the palmitoylation of DHHC17 and DHHC13 was also examined. As expected, both DHHC17 and DHHC13 were palmitoylated, as both proteins were captured by thiopropyl beads under conditions of hydroxylamine treatment (Fig. 2c, panel iii, lanes 4 and 6). Expression of DHHC17 or -13 had no appreciable impact on ClipR-59 expression, as comparable levels of Flag–ClipR-59 were detected in the samples (Fig. 2c, panel ii).

The data presented above suggest that DHHC17 and DHHC13 are likely ClipR-59 palmitoyltransferases. To further examine this, we next evaluated ClipR-59 palmitoylation with different doses of DHHC13 and DHHC17. As shown in Fig. 3a, DHHC17 promoted ClipR-59 palmitoylation in a dose-dependent manner (panel i, lanes 7 to 12) whereas DHHC13 had no appreciable impact on ClipR-59 palmitoylation until it reached the highest dose used in

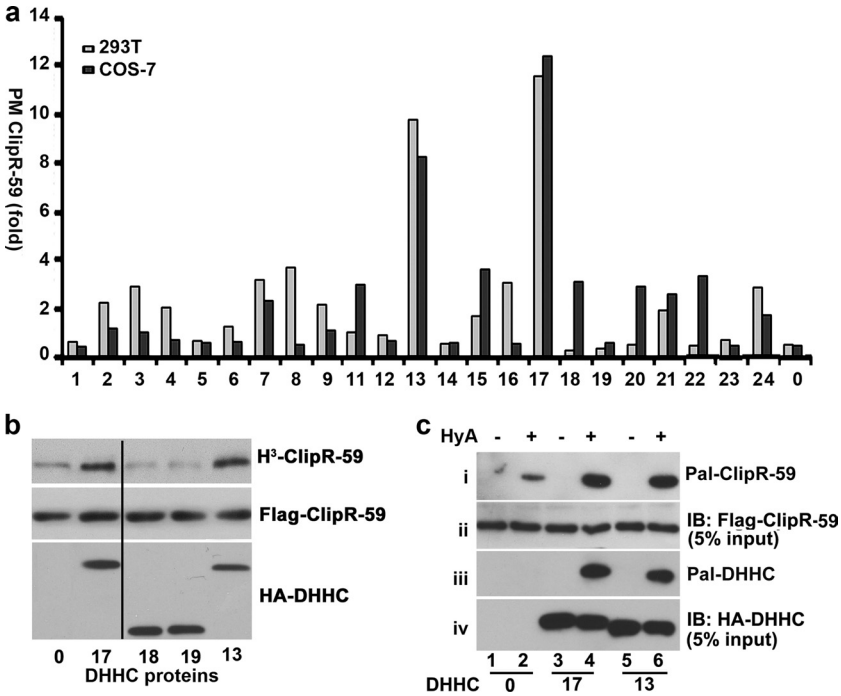

FIG 2 DHHC17 and DHHC13 mediate ClipR-59 palmitoylation. (a) The PM fractions were isolated from HEK293 and COS-7 cells that were cotransfected with equal amounts (0.5 μg) of Flag-tagged ClipR-59 and individual HA-tagged DHHC expression vectors and analyzed by Western blotting with anti-Flag antibody. The relative levels of Flag–ClipR-59 in membrane fractions from two independent experiments are presented. The levels of ClipR-59 at the membrane under control conditions were set at 1 (lane 0). (b) *In vivo* labeling of ClipR-59 with [^{3}H]palmitate in the presence of different DHHC proteins. The experiments were carried out as described for panel a, except that the cells were incubated with [^{3}H]palmitate overnight. Flag-tagged ClipR-59 was immunoprecipitated and exposed to X-ray film (top panel). The cellular levels of exogenously expressed ClipR-59 and HA-DHHC proteins are shown in middle and bottom panels, respectively. (c) Thiopropyl captivation assay (TPC assay) of ClipR-59 palmitoylation using S-acylated protein. HEK293 cells were transiently transfected as described for panel a, and TPC was performed as described in Materials and Methods. The proteins captured by thiopropyl beads were analyzed by Western blotting with anti-Flag antibody (i, detecting palmitoylated ClipR-59 [Pal-ClipR-59]) or anti-HA antibody (iii, detecting palmitoylated DHHC proteins). Panels ii and iv show the input levels of Flag–ClipR-59 and HA-DHHC proteins, respectively. HyA, hydroxylamine chloride; IB, immunoblot. The minus sign indicates that the samples were treated with sodium chloride.

these experiments (panel i, lanes 1 to 6). The difference between DHHC13 and DHHC17 in promoting ClipR-59 palmitoylation observed here was not a result of the differential levels of expression of DHHC13 and DHHC17, as DHHC13 appeared to express at a higher level than DHHC17 did (Fig. 3a, panel iii). In these experiments, we also assessed the autopalmitoylation of DHHC13 and DHHC17. The autopalmitoylation of each protein exhibited a dose-dependent increase (Fig. 3a, panel ii) in agreement with the view that DHHC17 autopalmitoylation is higher overall than that of DHHC13 (panel ii, compare lanes 2 to 6 with lanes 8 to 12). The autopalmitoylation of a DHHC protein is related to the DHHC protein palmitoyltransferase activity (21, 22). The higher level of DHHC17 autopalmitoylation likely reflects the notion that DHHC17 is a more active palmitoyltransferase. The reason for this is not clear at present but could be that DHHC13 contains a DQHC motif instead of the common DHHC motif in the DHHC protein catalytic domain (12). The quantified results of ClipR-59 palmitoylation under conditions of either DHHC13 or DHHC17 expression are presented in Fig. 3b, which clearly shows the differences between DHHC13 and DHHC17 with respect to their abilities to promote ClipR-59 palmitoylation.

Next, we carried out a coimmunoprecipitation assay with the lysates of HEK293 cells transiently cotransfected with Flag–ClipR-59 expression vector and HA-tagged DHHC17 or DHHC13 expression vectors to examine the interaction of ClipR-59 with DHHC13 and DHHC17. As shown in Fig. 3c, both DHHC17 and DHHC13 were recovered from the anti-Flag immunoprecipitates of HEK293 cell lysates that express Flag–ClipR-59 but not from those of the one without Flag–ClipR-59 expression (top panel, lanes 5 and 6 for DHHC17 and lanes 7 and 8 for DHHC13), indicating that both DHHC17 and DHHC13 are capable of interacting with ClipR-59. In these experiments, we also examined the association of ClipR-59 with DHHC7 and DHHC15. No DHHC7 was recovered from anti-Flag immunoprecipitates (Fig. 3c, top panel, lanes 1 and 2), and only a marginal amount of DHHC15 was seen in the anti-Flag immunoprecipitates (lanes 3 and 4). Quantitative analysis revealed that the amount of DHHC17 associated with anti-Flag–ClipR-59 beads was about 4.5-fold of the input level, whereas that of DHHC13 was about 2.0-fold, indicating that DHHC17 has the higher binding affinity for ClipR-59. When an enzyme catalyzes a reaction, it requires the enzyme to bind its substrate. The higher activity to promote ClipR-59 palmitoylation and the higher binding affinity for ClipR-59 argue that DHHC17 is likely the major ClipR-59 palmitoyltransferase in cells.

To determine whether DHHC17 mediates ClipR-59 palmitoylation at Cys534 and Cys535, the ability of DHHC17 to palmitoylate C2A2–ClipR-59 was assessed. As expected, while promoting wild-type ClipR-59 palmitoylation, DHHC17 had no impact on palmitoylation of C2A2–ClipR-59 (Fig. 3d, top panel, compare

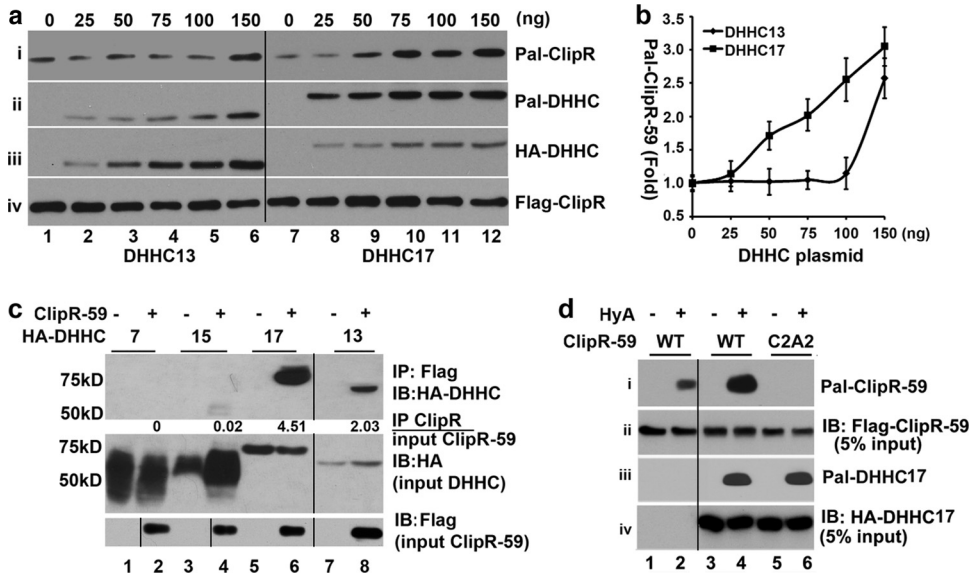

FIG 3 DHHC17 palmitoylates ClipR-59 with high activity. (a) Differential levels of palmitoylation of ClipR-59 by DHHC13 and DHHC17. HEK293 cells were transiently transfected with Flag–ClipR-59 using the indicated amount of HA-DHHC13 or DHHC17. At 36 h posttransfection, the total cell lysates were prepared for TPC assays. The thiopropyl beads with captured proteins were subjected to Western blot analysis with anti-Flag (i) and anti-HA (ii), respectively. The input levels of HA-DHHC proteins and ClipR-59 are shown in panels iii and iv, respectively. This experiment was repeated three times, and data from one representative experiment are shown. (b) Densitometry analysis of Western blot data shown in panel a from three independent experiments. The level of ClipR-59 palmitoylation with coexpression of DHHC proteins was set to a value of 1 after normalization to total cellular Flag–ClipR-59. Bars show means ± SD ($n = 3$). (c) Coimmunoprecipitation assay showing that DHHC17 has a higher affinity for interaction with ClipR-59. HEK293 cells were transiently cotransfected with Flag–ClipR-59 and the indicated HA-tagged DHHC expression vectors. At 36 h posttransfection, cell lysates were prepared and subjected to immunoprecipitation (IP) with anti-Flag antibody, and the presence of HA-tagged DHHC proteins in the anti-Flag immunoprecipitates was assessed by Western blotting (top panel). Input levels of individual DHHC proteins (middle panel) and Flag–ClipR-59 (bottom panel) are shown. The ratios of DHHC protein in anti-Flag immunoprecipitates and inputs are shown below the top panel. (d) TPC assay showing that DHHC17 promotes ClipR-59 palmitoylation at Cys534 and Cys535. The experiments were carried out as described for Fig. 2c, except that Flag-C2A2–ClipR-59 was also used. HyA, hydroxylamine chloride.

lanes 4 and 6), demonstrating that DHHC17 specifically palmitoylates ClipR-59 at Cys534 and Cys535.

MBD of ClipR-59 mediates the interaction between ClipR-59 and DHHC17. To further evaluate the association of ClipR-59 with DHHC17, a series of ClipR-59 deletion mutants were generated (Fig. 4a) and the affinity of each mutant to interact with DHHC17 was assessed in a coimmunoprecipitation assay. As shown in Fig. 4b, removal of either the ankyrin repeats or CAP-Gly domains had no impact on the interaction between DHHC17 and ClipR-59, suggesting that the ankyrin repeats and CAP-Gly domains are not required for the interaction between ClipR-59 and DHHC17. On the other hand, the mutants that lack MBD exhibited no detectable interaction with DHHC17 (Fig. 4c, top panel, compare lane 4 with lanes 6, 7, and 8), indicating that MBD of ClipR-59 mediates the association of ClipR-59 with DHHC17. In agreement with this view, removal of the first 90 amino acid residues had no impact on the interaction between ClipR-59 and DHHC17 (Fig. 4c, top panel, compare lanes 4 and 5). As additional studies, we also examined the interaction of ClipR-59 with DHHC13 and DHHC21. No interaction between DHHC21 and ClipR-59 was observed (Fig. 4c, top panel, compare lanes 3 and 4). Again, DHHC13 showed the lower affinity to interact with ClipR-59 (Fig. 4c, top panel, compare lanes 2 and 4). The differential interactions of ClipR-59 and its mutants with DHHC proteins were not a result of sample variations, as comparable levels of ClipR-59 and its mutants and DHHC proteins were detected in each sample (Fig. 4b and c, middle and bottom panels).

To determine whether the presence of the MBD of ClipR-59 is sufficient to mediate the interaction between ClipR-59 and DHHC17, a vector that expresses MBD-GFP fusion peptide was generated (Fig. 5a). Then a GST pulldown assay was carried out with the lysates from COS-7 cells that transiently transfected with GST-DHHC17 and GFP–ClipR-59 or GFP-MBD expression vectors. As shown in Fig. 5b, GFP-MBD exhibited a level of binding activity comparable to that seen with GST-DHHC17 (top panel, lanes 2 and 4). This binding was specific, as no ClipR-59 was found on GST beads (Fig. 5b, top panel, lanes 1, 3, and 5) and no GFP itself was found on GST-DHHC17 beads (compare lanes 5 and 6). These different observations are not a result of sample variations, as comparable levels of GFP fusion proteins (Fig. 5b, middle panel) and GST fusion proteins (bottom panel) were detected in each sample.

As a complementary approach, we also carried out a coimmunoprecipitation assay with anti-GFP antibody and with the lysates of COS-7 cells that transiently transfected with GFP-MBD and HA-DHHC17. As shown in Fig. 5c, HA-DHHC17 was readily detected in anti-GFP immunoprecipitates from the lysates of COS-7 cells that transiently transfected with GFP–ClipR-59 and HA-DHHC17 or with GFP-MBD and HA-DHHC17 but not with GFP and HA-DHHC17 (top panel, compare lanes 1, 2, and 3). The middle panel shows the cellular levels of HA-DHHC17, and the bottom panel shows the GFP fusion proteins in GFP immunoprecipitates. Together, these data demonstrate that MBD of ClipR-59 is sufficient to mediate the interaction between ClipR-59 and DHHC17.

In early studies, MBD was suggested to be the sole determinant

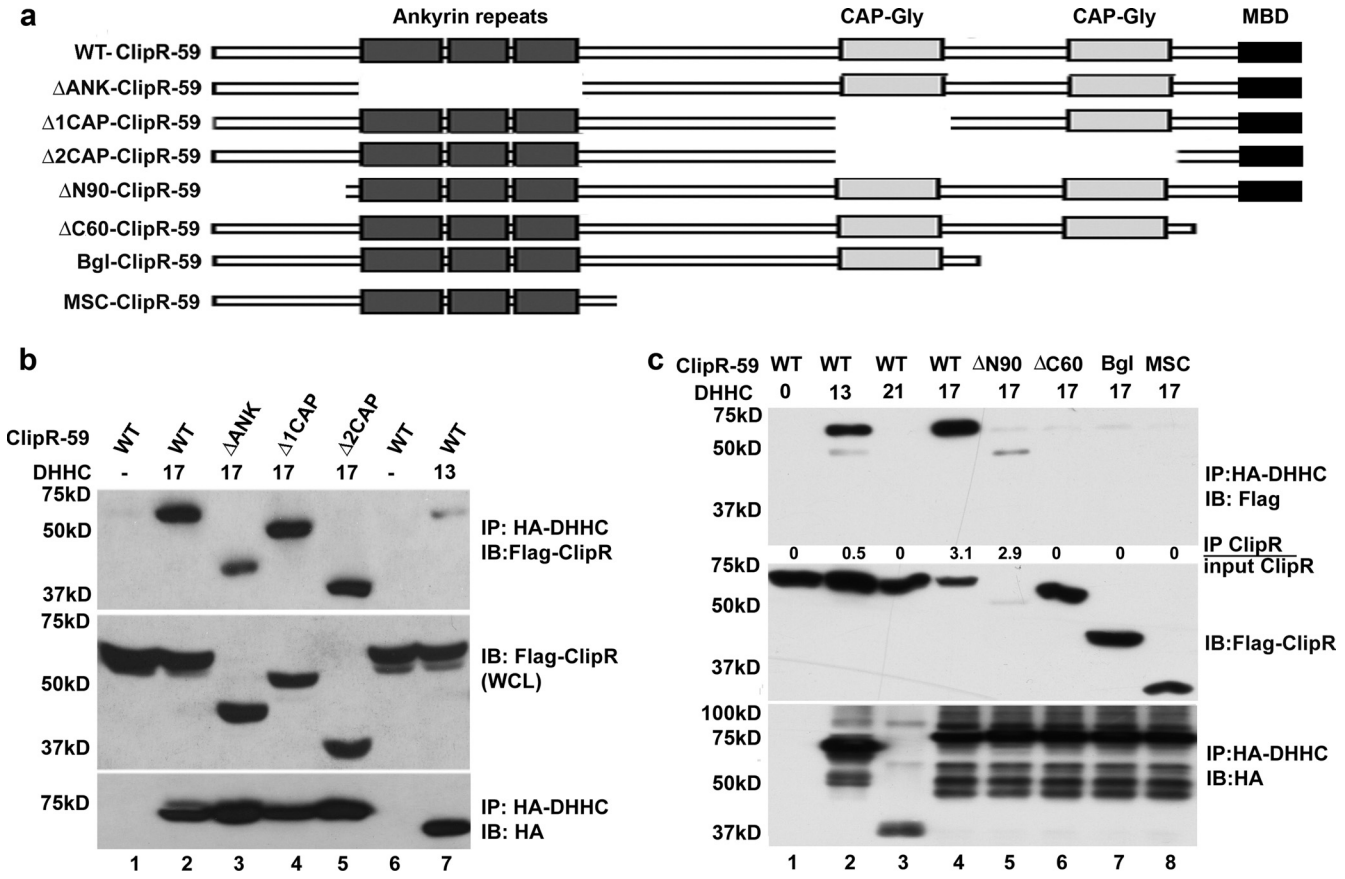

FIG 4 ClipR-59 MBD mediates the interaction between ClipR-59 and DHHC17-I. (a) Schematic presentation of ClipR-59 mutants used in the following experiments. The individual domains of ClipR-59 are indicated. Ank, ankyrin repeats; CAP-Gly, cytoplasmic linker glycine-rich domain; MBD, membrane binding domain. (b) Coimmunoprecipitation assay of lysates from HEK293 cells transiently expressed HA-DHHC17 and Flag-Clip-59 or mutants to show that ClipR-59 MBD mediates the interaction of ClipR-59 with DHHC17. Top panel, the presence of Flag–ClipR-59 (ClipR) and its mutants in HA-DHHC protein immunoprecipitates. Middle panel, the input levels of Flag–ClipR-59 and its mutants. Bottom panel, immunoprecipitated HA-DHHC proteins. WCL, whole-cell lysates. (c) The same as panel b, except that different ClipR-59 mutants were used. The ratios of ClipR-59 in anti-HA-DHHC immunoprecipitates and the input are shown in the bottom of top panel.

of ClipR-59 subcellular localization (10). To verify this, we compared the cellular localization of GFP-MBD with that of HA-tagged ClipR-59 in COS-7 cells. As shown in Fig. 5d, GFP-MBD exhibited cellular localization that was almost identical to that seen with HA-ClipR-59 (red). Overall, these results indicate that MBD of ClipR-59 is the important determinant for DHHC17–lipR-59 interactions. Both palmitoylated cysteine residues (Cys534 and Cys535) of ClipR-59 are within the MBD. Thus, the finding that ClipR-59 MBD mediates the association of ClipR-59 with DHHC17 supports the view of DHHC17 being a regulator of ClipR-59 palmitoylation.

DHHC17 modulates ClipR-59 PM association. Palmitoylation of ClipR-59 by DHHC17 implies that DHHC17 could modulate ClipR-59 subcellular localization. To test this, GFP-tagged ClipR-59 was cotransfected into COS-7 with a DHHC17 shRNA that has been shown to suppress DHHC17 expression (16). Then the cells were stained with anti-DHHC17-specific antibody, and the cellular localizations of GFP–ClipR-59 and DHHC17 (red) were visualized with fluorescence microscopy. As shown in Fig. 6a, altered ClipR-59 cellular localization (green), namely, a reduced level of ClipR-59 on the cell borders (membranes), was observed in the cells in which DHHC17 staining was absent (indicated by white arrows) compared with the ones that were positive for DHHC17 staining. The cells that were negative for DHHC17 staining represented the cells that expressed DHHC17 shRNA.

To further examine the impact of DHHC17 knockdown on ClipR-59 PM association, we also used another DHHC17 shRNA (TRCN0000137952). To ensure that both DHHC17 shRNA and GFP–ClipR-59 are expressed in the same cells, we constructed an expression vector that simultaneously expresses this DHHC17 shRNA and GFP–ClipR-59 (see Materials and Methods). Then we examined ClipR-59 subcellular localization when these vectors were introduced into COS-7 cells. As shown in Fig. 6b, compared with that in cells simultaneously expressing the luciferase shRNA and GFP–ClipR-59, an apparently decreased level of ClipR-59 on PM was observed in the DHHC17 shRNA- and GFP–ClipR-59-expressing cells (compare top and bottom panels), supporting the notion that DHHC17 promotes ClipR-59 membrane translocation.

To determine whether the decreased ClipR-59 PM association by DHHC17 shRNA is related to ClipR-59 palmitoylation and to verify that DHHC17 shRNA expression reduces ClipR-59 PM association, we next prepared total cell lysates, lipid rafts (or the

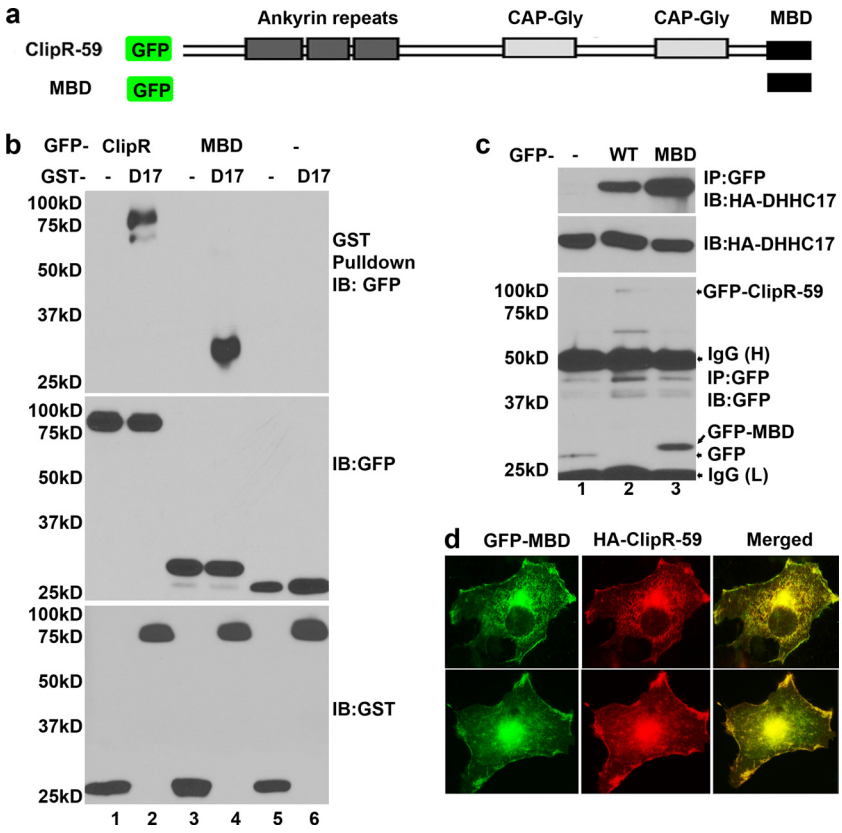

FIG 5 ClipR-59 MBD mediates the interaction between ClipR-59 and DHHC17-II. (a) Schematic presentation of ClipR-59 and MBD GFP fusion proteins. The individual domains of ClipR-59 are indicated. Ank, ankyrin repeats. CAP-Gly, cytoplasmic linker glycine-rich domain. MBD, membrane binding domain. (b) COS-7 cells were cotransfected with GST-DHHC17 (D17) and the indicated GFP–ClipR-59 expression vectors. GST-DHHC17 was then isolated with GST beads from total cell lysates and the proteins associated with GST beads were analyzed by Western blotting with anti-GFP antibody (top). The cellular levels of GFP–ClipR-59 and GST fusion proteins are shown in the middle panel and bottom panel, respectively. (c) Coimmunoprecipitation assay of COS-7 lysates expressing HA-DHHC7 and GFP fusion proteins. Top panel: Western blot of anti-GFP immunoprecipitates with anti-HA antibody to detect HA-DHHC17. Middle panel: the cellular level of HA-DHHC17. Bottom panel: Western blot of anti-GFP immunoprecipitates with anti-GFP antibody. The positions of IgG light chain (IgG-L), IgG heavy chain (IgG-H), GFP-MBD, GFP–ClipR-59, and GFP are indicated in the bottom panel. (d) Fluorescence images of COS-7 cells transfected with HA-ClipR-59 and GFP-MBD expression vectors and stained with anti-HA antibody followed by Cy3-conjugated monkey anti-mouse IgG. Two representative cell images are shown.

plasma membrane microdomain), and the PM fraction from COS-7 cells as described in the Fig. 6b legend and examined the levels of ClipR-59 palmitoylation, ClipR-59 in lipid rafts, and Akt on PM, respectively. We examined ClipR-59 in lipid rafts because a previous study suggested that the palmitoylation of ClipR-59 also targeted ClipR-59 into lipid rafts (10). Compared with that in luciferase shRNA-expressing cells, the levels of ClipR-59 palmitoylation in DHHC17 shRNA-expressing cells decreased by more than 70% (Fig. 6c, panel i, and d, left), with a corresponding reduction of the level of ClipR-59 in lipid rafts (Fig. 6c, panel ii, compare lanes 1 and 2; Fig. 6d, center left). Moreover, in agreement with the notion that ClipR-59 modulates Akt PM association, the level of Akt in PM was reduced in the cells that expressed DHHC17 shRNA (Fig. 6c, panel iv, compare lanes 1 and 2; Fig. 6d, center right). The DHHC17 shRNA was effective in suppressing DHHC17 expression, as a reduction of the DHHC17 protein level of more than 75% was seen in DHHC17 shRNA-expressing cells (Fig. 6c, panel vi, compare lanes 1 and 2; Fig. 6d, right). The differences in palmitoylated ClipR-59 and membrane-associated ClipR-59 and Akt between the cells expressing luciferase shRNA and DHHC17 shRNA were not a result of sample variations, as comparable levels of ClipR-59 (Fig. 6c, panel iii) and Akt (panel v) were observed. In the same setting, we examined the impact of forcing HA-DHHC17 protein expression on ClipR-59 membrane localization. In these experiments, exogenously expressed DHHC17 was detected with anti-HA antibody. In agreement with the notion that DHHC17 promotes ClipR-59 membrane localization, the density of GFP fluorescence on the cell surface was increased in HA-DHHC17-expressing cells (Fig. 6e, compare panel i and iv). DHHC17 expression is shown in panel ii. Collectively, these results demonstrate that DHHC17 promoted ClipR-59 palmitoylation, thereby modulating the PM association of ClipR-59 and Akt.

DHHC17 regulates insulin-dependent Glut4 membrane translocation in adipocytes. ClipR-59, in its membrane association-dependent manner, modulates Glut4 membrane translocation (2). Regulation of ClipR-59 membrane localization by DHHC17 implies that DHHC17 could modulate Glut4 membrane translocation. To test this, 3T3-L1 adipocytes were transduced with adenoviral vectors that express GFP (as a control) or HA-DHHC17. After these cells were serum starved overnight and treated with 10 nM insulin for 30 min, the PM fraction was pre-

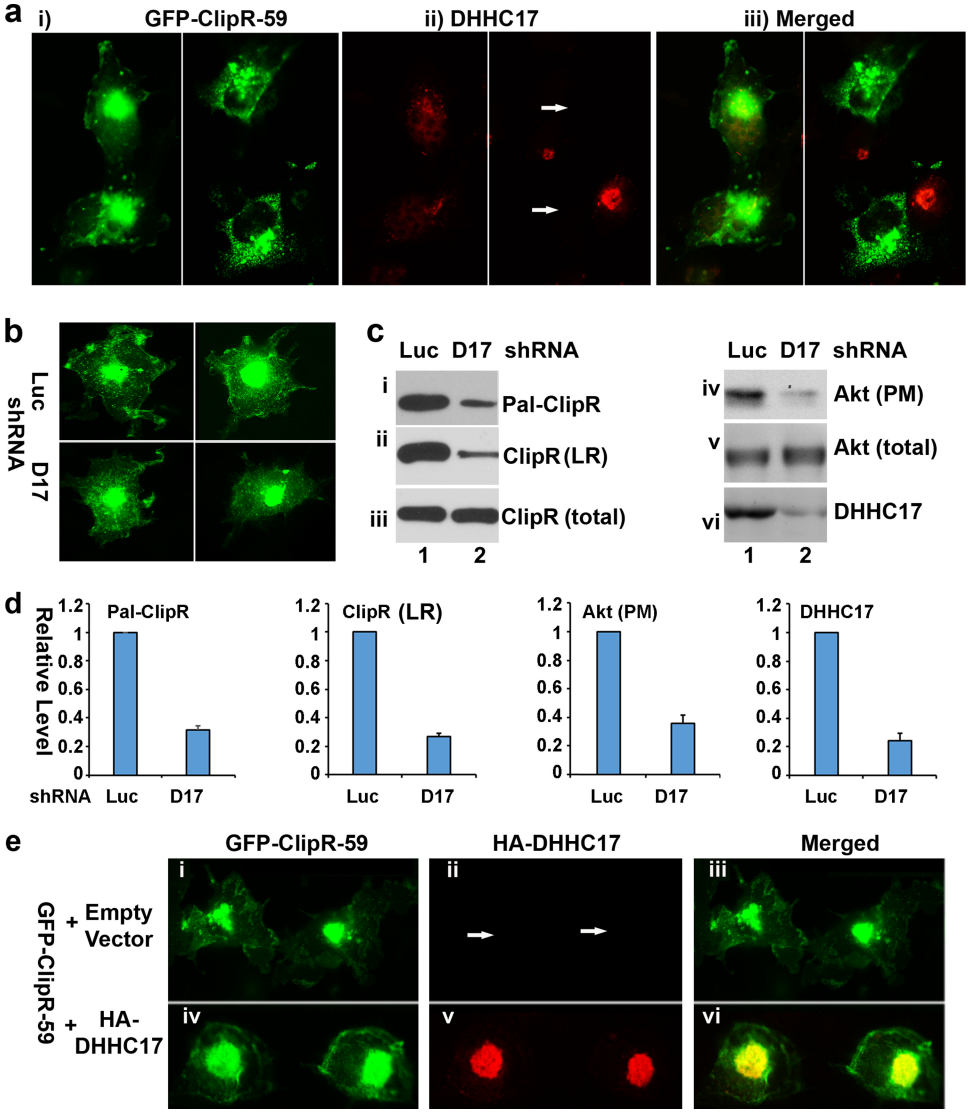

FIG 6 DHHC17 regulates ClipR-59 cellular localization. (a) COS-7 cells were transiently cotransfected with GFP–ClipR-59 expression vectors plus either luciferase shRNA (control) or DHHC17 shRNA. At 36 h posttransfection, the cells were fixed and stained with anti-DHHC17 antibody followed by Cy3-conjugated monkey anti-rabbit IgG antibodies. Data from two representative cells from each group of stained cells are shown. The arrows indicate the cells that lack DHHC17 staining. The brightness of the images was increased to highlight the absence of DHHC7 staining. (b) COS-7 cells were transiently cotransfected with expression vectors that simultaneously express GFP–ClipR-59 and either luciferase (Luc) shRNA (control) or DHHC17 shRNA. At 36 h posttransfection, the cells were fixed and the fluorescence images were captured using confocal fluorescence microscopy. Data from two representative cells from each group are shown. (c) TPC assay and subcellular fractionation assay of COS-7 cells used as described for panel b to show the levels of ClipR-59 palmitoylation (i) and of ClipR-59 in lipid rafts (LR) (ii) and in total cell lysates (iii) and the levels of Akt in PM (iv) and in total cell lysates (v) and of DHHC17 in total cell lysates (vi). These experiments were repeated three times with similar results, and data from one representative experiment are shown. (d) Densitometry analysis of palmitoylated ClipR-59, ClipR-59 and Akt in PM, and DHHC17 in total cell lysates from three independent experiments. The levels of each protein in control cells were set to a value of 1 after normalization to total cellular Akt. The bars show means ± SD ($n = 3$). (e) COS-7 cells were transiently cotransfected with GFP–ClipR-59 plus either empty vector (i, ii, and iii) or HA-DHHC17 expression vector (iv, v, and vi). At 36 h posttransfection, the cells were fixed and stained with anti-monoclonal-HA antibody followed by Cy3-conjugated monkey anti-mouse IgG antibody. Data from two representative cells from each group of stained cells are shown. Cells that lacked anti-HA staining are indicated by arrows.

pared to assess the levels of Glut4 and IRAP, the major cargos of Glut4 vesicles in PM. As shown in Fig. 7a, the amounts of both Glut4 and IRAP in PM fractions were induced by insulin, as expected (panel i and ii, compare lanes 1 and 2). Forcing expression of DHHC17 resulted in a further increase in the level of Glut4 and IRPA in PM under basal conditions (Fig. 7a, panel i and ii, respectively, compare lanes 1 and 3) and insulin-stimulated conditions (panel i and ii, compare lanes 2 and 4).

Next, we examined the levels of phospho-Akt in PM. As shown in Fig. 7a, compared with GFP expression, DHHC17 expression in 3T3-L1 adipocytes increased the amount of Akt in the PM fraction under both basal conditions (panel iii, compare lanes 1 and 3) and insulin-treated conditions (panel iii, compare lanes 2 and 4). The impact of DHHC17 on Akt is specific to the PM Akt, as no changes of total cellular phospho-Akt levels were observed (Fig. 7a, panel iv). The observed changes in Glut4 and Akt in the PM fraction

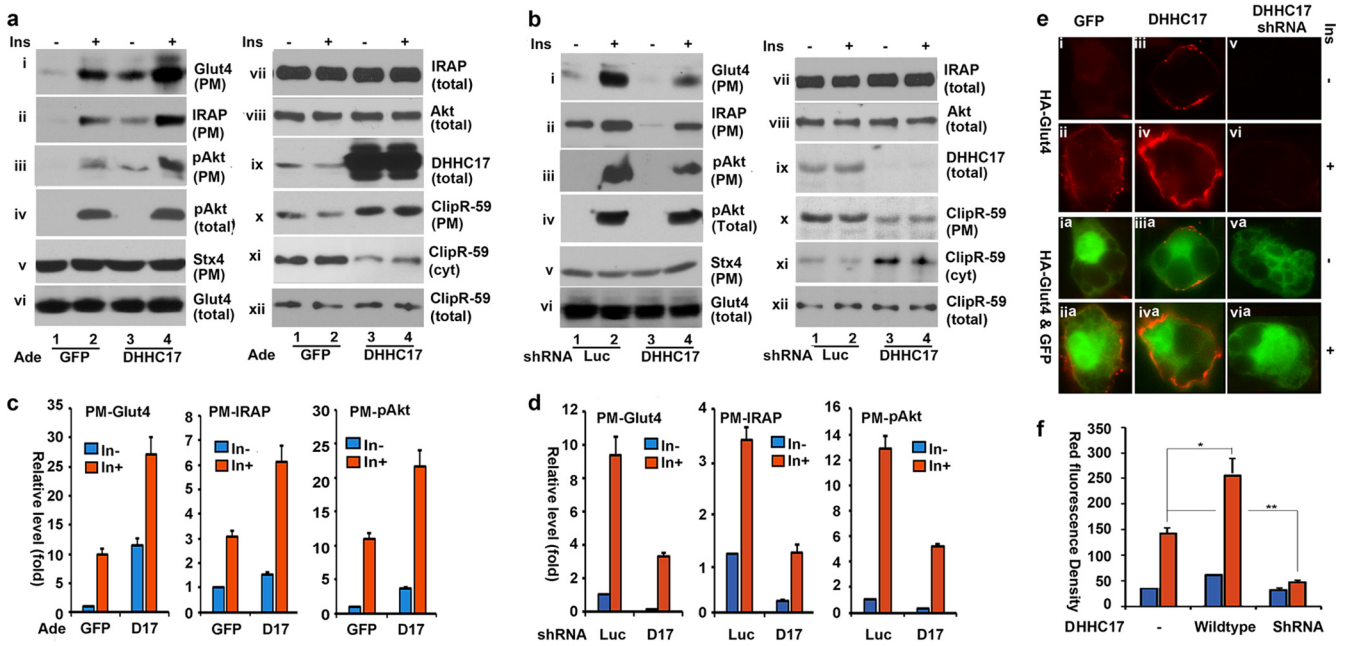

FIG 7 DHHC17 expression regulates Glut4 membrane translocation and Akt membrane association. (a) Fully differentiated 3T3-L1 adipocytes were transduced with GFP (control)- and DHHC17-expressing adenoviral vectors. The PM fractions were prepared after the cells were treated with 10 nM insulin for 30 min for Western blot analysis with anti-Glut4 (i), anti-IRAP (ii), anti-pAkt (iii), anti-syntaxin 4 (Stx4) (v), and anti-ClipR-59 (x) antibodies, respectively. The total cellular levels of pAkt (iv), Glut4 (vi), IRAP (vii), Akt (viii), DHHC17 (ix), and ClipR-59 in the cytosol fraction (xi) and total cell lysates (xii) are also shown. These experiments were repeated four times with similar results, and data from one representative experiment are shown. (b) The experiments were carried out essentially as described for panel a, except that the cells were transduced with adenoviral vectors expressing luciferase shRNA (Luc) and DHHC17 shRNA, respectively. These experiments were repeated three times with similar results, and data from one representative experiment are shown. Luc, luciferase. (c) The quantitative analysis of the levels of Glut4, IRAP, and pAkt in PM data shown in panel a. In these analyses, the levels of each protein were set to a value of 1 in the cells that express GFP without insulin treatments after normalization to syntaxin 4 in PM. Bars show means ± SD ($n = 3$). In all cases, P was < 0.05. Ade, adenoviral expression vector. (d) The same as panel c, except that the analyses are from panel b. Luc, luciferase; D17, DHHC17. (e) Immunocytochemistry of 3T3-L1 adipocytes cotransduced with adenoviral vector expressing HA-Glut4 along with that expressing GFP (control) (i), DHHC17 (ii), and DHHC17 shRNA (iii), respectively, with anti-HA antibody. The ratio of HA-Glut4-expressing adenoviral vectors and GFP-expressing adenoviral vectors was 5:1 to optimize HA-Glut4 expression in GFP-expressing cells. The cells were serum starved, treated with or without 10 nM insulin for 30 min, and immunostained with anti-HA antibody under nonpermeabilized conditions followed by Cy3-conjugated anti-mouse IgG antibody (red) and visualized with fluorescence microscopy. (f) Red fluorescence density in panel e after normalization to green fluorescence. Bar graphs show means ± SD ($n = 9$ cells). In all cases, P was <0.05.

were not a result of the effect of DHHC17 on ClipR-59 expression or sample variations, as comparable levels of syntaxin 4 in PM (Fig. 7a, panel v) and total cellular Glut4 (panel vi), IRAP (panel vii), and Akt (panel viii) were seen in each sample.

In these experiments, DHHC17 was sufficiently expressed (Fig. 7a, panel ix, compare lanes 1 and 3 or 2 and 4), and that expression was accompanied by increased ClipR-59 PM association (panel x, compare lanes 1 and 3 and lanes 2 and 4) and a decreased amount of ClipR-59 in cytosol (panel xi) without altering the total cellular level of ClipR-59 (panel xii), in agreement with the notion that DHHC17 promotes ClipR-59 palmitoylation and thereby PM association.

Next, 3T3-L1 adipocytes were transduced with adenoviral vectors that express a luciferase shRNA (as a control) or a DHHC17 shRNA, and the levels of Glut4, IRAP, and phospho-Akt in the PM fraction were examined. As shown in Fig. 7b, the expression of DHHC17 shRNA resulted in a marked decrease in the PM levels of Glut4 (panel i), IRAP (panel ii), and phospho-Akt (panel iii) but not in that of syntaxin 4 (panel v) under insulin-stimulated conditions, without altering the total cellular Glut4 (panel vi), IRAP (panel viii), phospho-Akt (panel iv), and Akt (panel viii) levels.

To determine whether the reduction of Glut4 and phospho-Akt levels in PM mediated by DHHC17 shRNA expression was related to the change in the ClipR-59 level in PM, the levels of ClipR-59 in PM were also examined. Consistent with the preceding observation (Fig. 6), expression of DHHC17 shRNA decreased the amount of ClipR-59 in PM (Fig. 7b, panel x, compare lanes 1 and 3 and lanes 2 and 4), with reciprocal changes in the cytosol (panel xi), without an alteration of total cellular ClipR-59 levels (panel xii). As expected, DHHC17 shRNA was effective in suppressing DHHC17 expression, as diminution of DHHC17 expression by more than 75% was observed in DHHC17 shRNA-expressing cells (Fig. 7b, panel ix, compare lanes 1 and 3 and lanes 2 and 4). Taken altogether, these data demonstrate that DHHC17, via its ability to modulate ClipR-59 PM association, regulates Akt PM association and Glu4 membrane translocation.

To further examine the impact of DHHC17 on Glut4 membrane translocation, we next assessed DHHC17 with respect to Glut4 membrane translocation with a HA-tagged Glut4 reporter. In the HA-Glut4 reporter, the HA epitope is inserted into the first exofacial loop of Glut4 (23). When the cells expressing HA-Glut4 were stained with anti-HA antibody under nonpermeabilized conditions, membrane-localized HA-Glut4, which is around the cell surface as a ring, thereby measuring the level of Glut4 on PM, was specifically detected. Specifically, HA-Glut4 was cointroduced either with GFP or with DHHC17 or DHHC17 shRNA into

3T3-L1 adipocytes via adenoviral gene transfer. After treatment with or without 10 nM insulin for 30 min, these cells were stained with anti-HA antibody under nonpermeabilized conditions. As shown in Fig. 7e, in control (GFP-expressing) adipocytes, marginal HA staining was detected without insulin treatment, and the density of the staining was increased about 5 times following insulin stimulation (Fig. 7e, panels i and ii, and f), indicative of insulin-dependent Glut4 membrane translocation. In the presence of DHHC17, significant membrane staining was observed (Fig. 7e, compare panels i and iii; Fig. 7f). Insulin stimulation further increased the level of HA staining, which was about 3 times more than that in control cells (Fig. 7e, compare panels ii and iv; Fig. 7f). In DHHC17 shRNA-expressing adipocytes, a markedly decreased level of Glut4 PM staining was observed under both basal and insulin-treated conditions (Fig. 7e, panels v and vi, and f) compared with that in the control cells (Fig. 7e, panels i and ii), suggesting that expression of DHHC17 shRNA suppressed Glut4 membrane translocation. It is noted that all of the adenoviral vectors used express GFP, which marked the transduced cells and the level of adenoviral vectors in each cell. As shown in Fig. 7e, all of the cells expressed comparable levels of GFP (compare panels ia, iia, iiia, and iva and panels va and via), an indication that these cells were equally transduced with adenoviruses. All together, these results demonstrate that DHHC17 is involved in Glut4 membrane translocation.

DISCUSSION

ClipR-59 modulates Akt cellular compartmentalization (2). This activity of ClipR-59 depends on ClipR-59 palmitoylation at Cys534/535 (Fig. 1). In eukaryotes, protein palmitoylation at cysteine residue is catalyzed by a family of DHHC protein palmitoyltransferases characterized by sharing a common DHHC motif. There are 23 DHHC palmitoyltransferases in the mouse genome. We thus examined the ability of each of the 23 DHHC palmitoyltransferases to promote ClipR-59 palmitoylation and found that both DHHC13 and DHHC17 were capable of palmitolylating ClipR-59 at the highest amplitude (Fig. 2).

Among mammalian DHHC proteins, DHHC13 and DHHC17 are closely related palmitoyltransferases, as they share high sequence homology (76% sequence identity) and have identical functional domains, including 5 ankyrin repeats, a DHHC motif, and 6 transmembrane domains (24, 25). In this regard, the finding that both DHHC13 and DHHC17 promote ClipR-59 palmitoylation is not merely coincidence. Instead, it emphasizes the effectiveness of our screening procedure to identify ClipR-59 palmitoyltransferase.

While both DHHC13 and DHHC17 were capable of promoting ClipR-59 palmitoylation, DHHC17 appeared more active in palmitoylating ClipR-59 with a high affinity to bind ClipR-59 (Fig. 3). This led us to the conclusion that DHHC17 is likely the major ClipR-59 palmitoyltransferase *in vivo*. Therefore, our studies were primarily focused on DHHC17. In an attempt to understand the interaction between ClipR-59 and DHHC17, we created a panel of ClipR-59 mutants and found that MBD of ClipR-59 mediates the interaction between ClipR-59 and DHHC17 (Fig. 4). ClipR-59 MBD is the sole determinant for ClipR-59 targeting to the PM (Fig. 5; see also references 1 and 10). Thus, the finding that ClipR-59 MBD mediates DHHC17–lipR-59 interaction is consistent with this notion.

Since our initial study showed that exogenous expression of DHHC17 increased ClipR-59 PM association (Fig. 2), we next examined the impact of DHHC17 shRNA on ClipR-59 PM association. In both COS-7 cells (Fig. 6) and 3T3-L1 adipocytes (Fig. 7), expression of DHHC17 shRNA reduced the level of ClipR-59 associated with PM, providing compelling evidence that DHHC17 is a ClipR-59 palmitoyltransferase. In this study, we found that DHHC17 is localized in the Golgi compartment as previously described (26). This implies that ClipR-59 undergoes palmitoylation in the Golgi compartment, in agreement with the notion that the Golgi compartment is a major site where protein palmitoylation occurs (27).

ClipR-59, by recruiting phospho (active)-Akt to the PM, promotes Glut4 membrane translocation (2). Because ClipR-59 recruitment of Akt to the PM requires ClipR-59 PM association mediated by palmitoylation (Fig. 1), we anticipated that DHHC17 would influence Akt PM association and Glut4 membrane translocation. Supporting this notion, we found that expression of DHHC17 shRNA diminished whereas expression of DHHC17 cDNA increased the PM-associated Akt following insulin stimulation (Fig. 7). Furthermore, the fact that DHHC17 affects the level of pAkt in PM but not that of total cellular phospho-Akt (Fig. 7a and b) emphasizes the notion that DHHC17 modulates Akt PM association via regulation of ClipR-59 PM association.

The regulation of Akt PM association by DHHC17 via promoting ClipR-59 palmitoylation is apparently important for insulin-dependent Glut4 membrane translocation, as expression of DHHC17 shRNA reduced whereas that of DHHC17 cDNA increased the level of Glut4 on PM in 3T3-L1 adipocytes (Fig. 7).

In mammals, the regulation of blood glucose levels is achieved, in part, through insulin-dependent Glut4 translocation to the PM in adipocytes and muscle cells. Impaired insulin-dependent Glut4 membrane translocation is the primary cause of hyperglycemia, the primary clinical symptom of type II diabetes mellitus. The finding that DHHC17 modulates insulin-dependent Glut4 membrane translocation argues that DHHC17 is potentially involved in diabetes. Recently, DHHC17 was found to regulate beta cell survival and insulin secretion (28). Accordingly, it was proposed that DHHC17 is a diabetes candidate gene. Our finding that DHHC17 is involved in Glut4 membrane translocation further emphasizes this notion.

It is also noteworthy that ClipR-59 is potentially involved in the regulation of tumor necrosis factor alpha (TNF-α) signaling (29) and neuronal innervations (30). Thus, in the future it would be interesting to know whether DHHC17 could also modulate TNF-α signaling and neuron growth.

In summary, we have identified DHHC17 as a ClipR-59 palmitoyltransferase and demonstrated that DHHC17 modulates insulin-dependent Glut4 membrane translocation. These results suggest that DHHC17 expression or activity would be important for preventing the development of type II diabetes. Further studies of DHHC17 knockout mice will provide more evidence for this notion.

ACKNOWLEDGMENTS

This work was supported by NIH grant RO1 DK084319 to K.D.

We are grateful for the generous gifts of HA-tagged murine DHHC protein expression vectors from Masaki Fukata (National Institute for Physiological Sciences, Okazaki, Japan) and of internally HA-tagged Glut4 expression vector from Samuel W. Cushman (National Institute of

Diabetes and Digestive and Kidney Diseases, Bethesda, Maryland). We also thank Sarwat Cheema for technical assistance.

REFERENCES

1. **Perez F, Pernet-Gallay K, Nizak C, Goodson HV, Kreis TE, Goud B.** 2002. CLIPR-59, a new trans-Golgi/TGN cytoplasmic linker protein belonging to the CLIP-170 family. J. Cell Biol. **156:**631–642.
2. **Ding J, Du K.** 2009. ClipR-59 interacts with Akt and regulates Akt cellular compartmentalization. Mol. Cell. Biol. **29:**1459–1471.
3. **Sakamoto K, Holman GD.** 2008. Emerging role for AS160/TBC1D4 and TBC1D1 in the regulation of GLUT4 traffic. Am. J. Physiol. Endocrinol. Metab. **295:**E29–E37.
4. **Ren W, Cheema S, Du K.** 2012. The association of ClipR-59 protein with AS160 modulates AS160 protein phosphorylation and adipocyte Glut4 protein membrane translocation. J. Biol. Chem. **287:**26890–26900.
5. **Bogan JS.** 2012. Regulation of glucose transporter translocation in health and diabetes. Annu. Rev. Biochem. **81:**507–532.
6. **Huang S, Czech MP.** 2007. The GLUT4 glucose transporter. Cell Metab. **5:**237–252.
7. **Minokoshi Y, Kahn CR, Kahn BB.** 2003. Tissue-specific ablation of the GLUT4 glucose transporter or the insulin receptor challenges assumptions about insulin action and glucose homeostasis. J. Biol. Chem. **278:**33609–33612.
8. **Graham TE, Kahn BB.** 2007. Tissue-specific alterations of glucose transport and molecular mechanisms of intertissue communication in obesity and type 2 diabetes. Horm. Metab. Res. **39:**717–721.
9. **Kotani K, Peroni OD, Minokoshi Y, Boss O, Kahn BB.** 2004. GLUT4 glucose transporter deficiency increases hepatic lipid production and peripheral lipid utilization. J. Clin. Invest. **114:**1666–1675.
10. **Lallemand-Breitenbach V, Quesnoit M, Braun V, El Marjou A, Pous C, Goud B, Perez F.** 2004. CLIPR-59 is a lipid raft-associated protein containing a cytoskeleton-associated protein glycine-rich domain (CAP-Gly) that perturbs microtubule dynamics. J. Biol. Chem. **279:**41168–41178.
11. **Mitchell DA, Vasudevan A, Linder ME, Deschenes RJ.** 2006. Protein palmitoylation by a family of DHHC protein S-acyltransferases. J. Lipid Res. **47:**1118–1127.
12. **Greaves J, Chamberlain LH.** 2011. DHHC palmitoyl transferases: substrate interactions and (patho)physiology. Trends Biochem. Sci. **36:**245–253.
13. **Korycka J, Lach A, Heger E, Boguslawska DM, Wolny M, Toporkiewicz M, Augoff K, Korzeniewski J, Sikorski AF.** 2012. Human DHHC proteins: a spotlight on the hidden player of palmitoylation. Eur. J. Cell Biol. **91:**107–117.
14. **Fukata M, Fukata Y, Adesnik H, Nicoll RA, Bredt DS.** 2004. Identification of PSD-95 palmitoylating enzymes. Neuron **44:**987–996.
15. **Huang K, Yanai A, Kang R, Arstikaitis P, Singaraja RR, Metzler M, Mullard A, Haigh B, Gauthier-Campbell C, Gutekunst CA, Hayden MR, El-Husseini A.** 2004. Huntingtin-interacting protein HIP14 is a palmitoyl transferase involved in palmitoylation and trafficking of multiple neuronal proteins. Neuron **44:**977–986.
16. **Huang K, Sanders S, Singaraja R, Orban P, Cijsouw T, Arstikaitis P, Yanai A, Hayden MR, El-Husseini A.** 2009. Neuronal palmitoyl acyl transferases exhibit distinct substrate specificity. FASEB J. **23:**2605–2615.
17. **Du K, Herzig S, Kulkarni RN, Montminy M.** 2003. TRB3: a tribbles homolog that inhibits Akt/PKB activation by insulin in liver. Science **300:**1574–1577.
18. **Fernández-Hernando C, Fukata M, Bernatchez PN, Fukata Y, Lin MI, Bredt DS, Sessa WC.** 2006. Identification of Golgi-localized acyl transferases that palmitoylate and regulate endothelial nitric oxide synthase. J. Cell Biol. **174:**369–377.
19. **Forrester MT, Hess DT, Thompson JW, Hultman R, Moseley MA, Stamler JS, Casey PJ.** 2011. Site-specific analysis of protein S-acylation by resin-assisted capture. J. Lipid Res. **52:**393–398.
20. **Ren W, Jhala US, Du D.** 2013. Proteomic analysis of protein palmitoylation in adipocytes. Adipocyte **2:**17–28.
21. **Roth AF, Feng Y, Chen L, Davis NG.** 2002. The yeast DHHC cysteine-rich domain protein Akr1p is a palmitoyl transferase. J. Cell Biol. **159:**23–28.
22. **Ohno Y, Kashio A, Ogata R, Ishitomi A, Yamazaki Y, Kihara A.** 2012. Analysis of substrate specificity of human DHHC protein acyltransferases using a yeast expression system. Mol. Biol. Cell **23:**4543–4551.
23. **Dawson K, Aviles-Hernandez A, Cushman SW, Malide D.** 2001. Insulin-regulated trafficking of dual-labeled glucose transporter 4 in primary rat adipose cells. Biochem. Biophys. Res. Commun. **287:**445–454.
24. **Ducker CE, Stettler EM, French KJ, Upson JJ, Smith CD.** 2004. Huntingtin interacting protein 14 is an oncogenic human protein: palmitoyl acyltransferase. Oncogene **23:**9230–9237.
25. **Yanai A, Huang K, Kang R, Singaraja RR, Arstikaitis P, Gan L, Orban PC, Mullard A, Cowan CM, Raymond LA, Drisdel RC, Green WN, Ravikumar B, Rubinsztein DC, El-Husseini A, Hayden MR.** 2006. Palmitoylation of huntingtin by HIP14 is essential for its trafficking and function. Nat. Neurosci. **9:**824–831.
26. **Ohno Y, Kihara A, Sano T, Igarashi Y.** 2006. Intracellular localization and tissue-specific distribution of human and yeast DHHC cysteine-rich domain-containing proteins. Biochim. Biophys. Acta **1761:**474–483.
27. **Rocks O, Gerauer M, Vartak N, Koch S, Huang ZP, Pechlivanis M, Kuhlmann J, Brunsveld L, Chandra A, Ellinger B, Waldmann H, Bastiaens PI.** 2010. The palmitoylation machinery is a spatially organizing system for peripheral membrane proteins. Cell **141:**458–471.
28. **Berchtold LA, Storling ZM, Ortis F, Lage K, Bang-Berthelsen C, Bergholdt R, Hald J, Brorsson CA, Eizirik DL, Pociot F, Brunak S, Storling J.** 2011. Huntingtin-interacting protein 14 is a type 1 diabetes candidate protein regulating insulin secretion and beta-cell apoptosis. Proc. Natl. Acad. Sci. U. S. A. **108:**E681–E688.
29. **Fujikura D, Ito M, Chiba S, Harada T, Perez F, Reed JC, Uede T, Miyazaki T.** 2012. CLIPR-59 regulates TNF-alpha-induced apoptosis by controlling ubiquitination of RIP1. Cell Death Dis. **3:**e264. doi:10.1038/cddis.2012.3.
30. **Couesnon A, Offner N, Bernard V, Chaverot N, Backer S, Dimitrov A, Perez F, Molgo J, Bloch-Gallego E.** 2013. CLIPR-59: a protein essential for neuromuscular junction stability during mouse late embryonic development. Development **140:**1583–1593.